Eur. Phys. J. Plus (2016) **131**: 418
DOI 10.1140/epjp/i2016-16418-6

THE EUROPEAN PHYSICAL JOURNAL PLUS

Regular Article

Multi-PV technologies method for parameters estimation of two-diode model

Souhir Sallem, Amal Marrekchi[a], Soulaymen Kammoun, and Mohamed Ben Ali Kammoun

Commande des Machines Électriques et Réseaux de Puissance (CMERP), National Engineering School of Sfax ENIS, Sfax, Tunisia

Received: 22 April 2016 / Revised: 8 November 2016
Published online: 2 December 2016 –

Abstract. Researches are showing that photovoltaic cell equivalent model parameters are not constant and are sensitive to climatic conditions changes. An improved algorithm for multi-photovoltaic cells manufacturing technologies to estimate those parameters is presented in this paper. The method allows a dynamic model for the PV cell according to different climatic conditions. This method shows a better performance of the model for several technologies (poly-crystalline, mono-crystalline and amorphous) of the PV module. Simulated I-V curves are compared to experimental characteristics and other estimation methods for different PV modules and different technologies. Some considerations about the impact of the variations of these resistances on the PV module performance are drawn.

Nomenclature

I_{pv}	PV cell current	I_{phSTC}	Current generated by the incidence of light at STC
I_{ph}	Light-generated current	G	Solar irradiance
I_{D1}	Diode 1 current	T_j	P-N junction temperature in PV cell
I_{D2}	Diode 2 current	I_{01}	Diode 1 reverse saturation current
R_s	Series resistance	I_{02}	Diode 2 reverse saturation current
R_p	Shunt resistance	V_T	Thermal voltage,
V_{pv}	PV cell voltage	a_1	Diode 1 ideality constant ($a_1 = 1$)
α_{sc}	Temperature coefficient of short-circuit current	a_2	Diode 2 ideality constant ($a_2 = 2$)
β_{oc}	Temperature coefficient of open-circuit voltage	q	Electron charge ($1.60217646 \cdot 10^{-19}$ C)
STC	Standard Test Conditions	k	Boltzmann constant ($1.3806503 \cdot 10^{-23}$ J/K)

1 Introduction

Recently, a major priority is the development of green energy, especially solar energy. This energy is becoming popular due to its lower pollution compared to fuels. The characteristics of a PV panel are essential for designing and dimensioning a PV power supply. In the literature, researches focus on refining PV models to encourage the developing of new high-performance conversion systems and the prediction of the behavior of the system under different climatic conditions. Many models are proposed: starting from the one-diode model, to the RS model, the RP model as well as the two-diode model and three-diode model [1] and [2]. There is another important aspect of the PV simulation. It is the estimation of the values of components and parameters of the model. Usually, the manufacturer datasheets give only the open-circuit voltage, short-circuit current, MPP current voltage and power. These STC parameters are not sufficient to extract the optimal parameters for various climatic conditions.

[a] e-mail: amal.marrekchi@gmail.com (corresponding author)

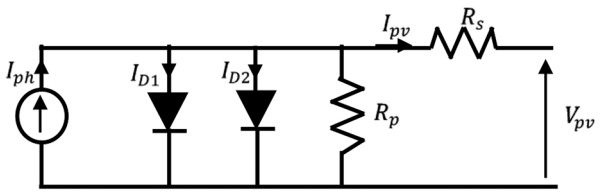

Fig. 1. Double-diode circuit model.

In this field, many researches treat the five-parameter-for-single-diode model to describe analytically *I-V* characteristic of a PV module for different conditions [3–6]. The parameters of the equivalent electrical circuit are estimated by solving system equations based on data commonly issued by manufacturers in STC [7–10]. In addition, serial and shunt resistances are then supposed constant for different climatic conditions.

A new five-parameter estimation is presented in this paper to compute dynamic internal parameters, namely I_{ph}, I_{01}, I_{02}, R_s and R_p based on the short circuit, the open circuit and the maximum power points of the *I-V* curve for different irradiances and temperatures. The rest of the paper is organized as follows; a two-diode model is developed in sect. 2. Section 3 describes the dynamic five-parameter estimation algorithm. Simulation results are given and compared to experimental results in sect. 4. A conclusion is presented in the last section.

2 PV cell modelling

The two-diode PV cell model is used in this paper since it improves the accuracy of the PV system and overcomes the disadvantages of the single-diode model [10]. The corresponding electrical model of the photovoltaic cell includes two diodes in parallel with the current source and a shunt resistance in addition to a series resistance. The two diodes represent the PN junction polarization phenomena [11–14]. The two resistors have some effects on the *I-V* characteristics of the cell [15]. The series resistance is the internal resistance of the PV cell; it depends on the resistance of the semiconductor. The shunt resistance is due to leakage at the junction [15–17]. The equivalent circuit of the two-diode model is presented in fig. 1 [10,18]. Equation (1) gives the currents in diode D1 and D2.

$$\begin{cases} I_{D1} = I_{o1}\left[\exp\left(\dfrac{V_{pv}+I_{pv}R_s}{a_1 V_T}\right)-1\right], \\ \\ I_{D2} = I_{o2}\left[\exp\left(\dfrac{V_{pv}+I_{pv}R_s}{a_2 V_T}\right)-1\right]. \end{cases} \tag{1}$$

Reverse saturation currents in D1 and D2 are given by eq. (2) [8],

$$\begin{cases} I_{01} = \dfrac{I_{sc\_STC}+\alpha_{sc}\Delta T}{\exp\left[\frac{V_{oc\_STC}+\beta_{oc}\Delta T}{a_1 V_T}\right]-1}, \\ \\ I_{02} = \dfrac{I_{sc\_STC}+\alpha_{sc}\Delta T}{\exp\left[\frac{V_{oc\_STC}+\beta_{oc}\Delta T}{a_2 V_T}\right]-1}. \end{cases} \tag{2}$$

$V_T = k\frac{T}{q}$ is the thermal voltage, a_1 and a_2 represent diodes ideality constants according to [19] and T is the temperature of the PN junction in K. The current generated by the light incidence is given by eq. (3),

$$I_{ph} = (I_{ph_{STC}} + \alpha_{sc}\Delta T)\frac{G}{G_{STC}}. \tag{3}$$

The application of Kirchhoff law yields the expression of the cell output current eq. (4),

$$I_{pv} = I_{ph} - I_{D1} - I_{D2} - \frac{(V_{pv}+I_{pv}R_s)}{R_p}. \tag{4}$$

As a PVG is made essentially by grouping N_p parallel branches where each branch is composed by N_s serial modules of N_{sc} PV cells, the output global PVG current is deduced from eq. (4) by substituting I_{D1} and I_{D2} from eq. (1) [17],

$$I_{pvg} = N_p I_{ph} - N_p I_{o1}\left[\exp\left(\frac{V_{pvg}+\frac{N_s}{N_p}R_s I_{pvg}}{N_s N_{sc} a_1 V_T}\right)-1\right] - N_p I_{o2}\left[\exp\left(\frac{V_{pvg}+\frac{N_s}{N_p}R_s I_{pvg}}{N_s N_{sc} a_2 V_T}\right)-1\right] - \frac{(V_{pvg}\frac{N_p}{N_s}+I_{pvg}R_s)}{R_p}. \tag{5}$$

3 New five-parameters estimation method

The manufacturers always provide I_{MP}, V_{MP}, V_{OC} and I_{sc} at STC. The series and shunt resistors are deduced from these values and are supposed constant for all operating conditions [19].

The algorithm of parameters estimation hereafter called "STC algorithm" uses an iterative method, which can be divided into 4 steps.

- Step 1. Compute the initial values of R_s, R_p, I_{ph}, I_{01} and I_{02} from the datasheet (V_{oc}, V_{mp}, I_{sc}, I_{mp}, V_{mp}) using eq. (2) and eq. (3) in STC, R_s, R_p is then deduced, eq. (6),

$$\begin{cases} R_s = 0, \\ R_{po} = \left(\dfrac{V_{mp}}{I_{sc} - I_{mp}}\right) - \left(\dfrac{V_{oc} - V_{mp}}{I_{mp}}\right), \end{cases} \tag{6}$$

  where R_{po} is the difference between the slopes of two line segments: the first is the slope between I_{sc} and I_{mp}, and the second is the slope between V_{mp} and V_{oc}.
- Step 2. For each iteration, the value of R_p is computed using eq. (7),

$$R_p = \frac{V_{mp} + I_{mp}R_s}{I_{ph} - I_0\left[\exp\left(\frac{V_{PV}+R_sI_{PV}}{a_1V_T}\right) + \exp\left(\frac{V_{PV}+R_sI_{PV}}{a_2V_T}\right) - 2\right] - (P_{max\_D}/V_{mp})}. \tag{7}$$

- Step 3. Compute $I_{pv} = f(V_{pv})$ using the Newton-Raphson method and deduce the computed maximum PV power.
- Step 4. If $|P_{max-c} - P_{max-D}| > \varepsilon$, the margin from the provided manufacturer power P_{max-D}, then go to step 2; else, R_s and R_p are held for the PV model.
  The tolerance ε is selected equal to 0.05% for poly-crystalline, 0.25% for mono-crystalline and 1% for amorphous technology modules.
  The obtained R_s and R_p are then considered constant for PV modeling under different climatic conditions.

The work developed in this paper is a new five-parameter model estimation method for the two-diode model where the estimated parameters are computed based on I_{MP}, V_{MP}, open-circuit voltage V_{OC} and short-circuit current I_{sc} for various climatic conditions. This algorithm ensures R_s and R_p readjustment *versus* temperature and irradiance perturbations. The obtained internal parameters are consequently dynamic and change *versus* climatic conditions. Figure 2 gives the flowchart of the developed estimation method called "dynamic algorithm" [16].

4 Simulation results and discussion

The estimated R_s and R_p using the dynamic algorithm are adopted to model three types of modules technologies: poly-crystalline, mono-crystalline and amorphous. Table 1 shows the manufacturer's electrical values in STC for the three different types. Tables 2 and 3 show parameters and essential points values of poly-crystalline modules MSX60 and KC-200GT compared with results of two methods developed respectively in [10] and [18] in STC. Table 4 shows computed essential parameters of the *I-V* curve of KC-200GT at conditions $G = 800\,\mathrm{W/m^2}$ and $T = 20\,^\circ\mathrm{C}$ compared with datasheet values and those obtained from computing the model using R_s and R_p given in [10]. Figure 3 shows the developed model based on the dynamic algorithm of MSX60 compared with datasheet values and developed models in [10] and [18] for several temperatures. Figures 4 and 5 show the simulated *I-V* curves using the proposed model of KC-200GT and the manufacturing data, respectively, for several temperatures and solar irradiances. Table 5 and table 6 summarize the values of shunt and series resistances R_p and R_s of the developed model computed for each climatic condition using the dynamic algorithm, respectively, recorded in figs. 4 and 5.

The proposed model and models of refs. [10] and [18] exhibit similar results for the STC. This is expected because the three models have almost the same values of calculated parameters of the equivalent model. In tables 2 and 3, the error of the values of parameters of MSX 60 and KC-200GT does not exceed 0.4%. The *I-V* curves of the three models in STC are close to the manufacturing curve in fig. 3. However, for $G = 800\,\mathrm{W/m^2}$ and $T = 20\,^\circ\mathrm{C}$, the proposed model using the dynamic algorithm gives more accuracy than the other developed models in [10]; for example in table 4 the error between the maximum power of ref. [10] and the datasheet value is around 3.6% but this error using the dynamic algorithm is equal to 0.0032%. Moreover, the dynamic algorithm offers *I-V* curves close to the datasheet values (figs. 3, 4 and 5). We can conclude that the model obtained from the dynamic algorithm is more accurate and close to the manufacturing data. According to tables 5 and 6, the series and shunt resistance vary *versus* climatic conditions based on the dynamic algorithm, which allows us to obtain *I-V* curves close to experimental data. In the rest of the paper we will evaluate the model provided by the dynamic algorithm and the manufacturing data for the mono-crystalline and amorphous technologies.

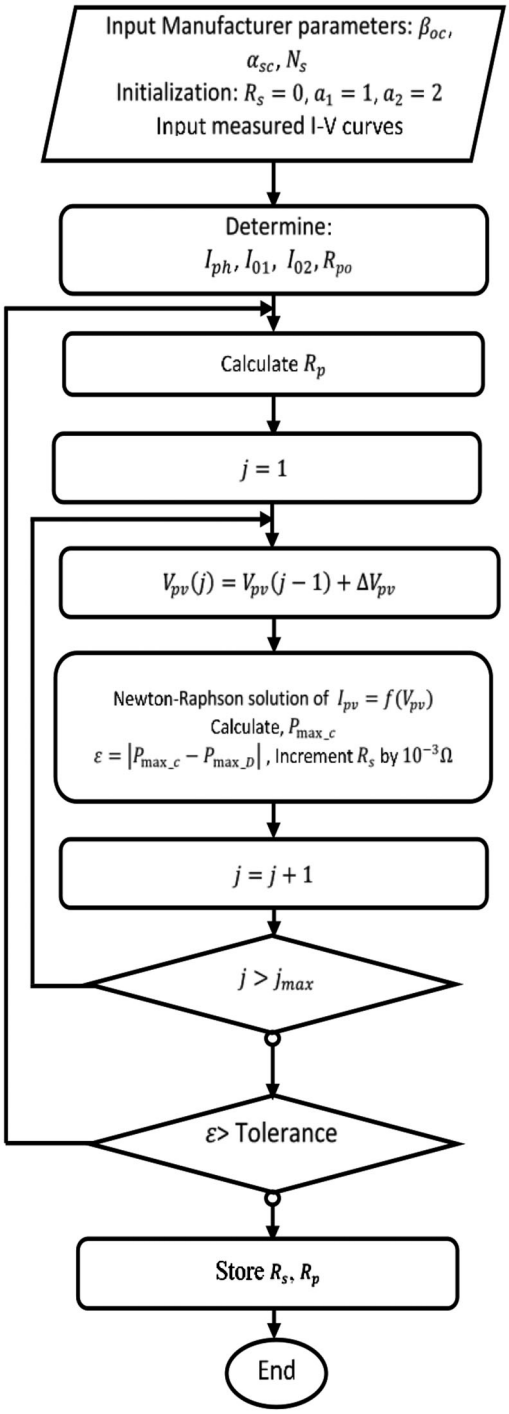

Fig. 2. Flowchart of the dynamic algorithm for the PV parameters estimation [16].

Table 7 shows parameters values of mono-crystalline modules (ISF-240 and SW280) obtained from the dynamic model at STC. Table 8 shows the computed essential parameters of mono-crystalline modules compared with manufacturing values at $G = 800\,\mathrm{W/m^2}$ and $T = 20\,^\circ\mathrm{C}$. Table 9 shows the parameters values and the essential point of the amorphous module compared to the manufacturing values for two conditions: STC and $G = 800\,\mathrm{W/m^2}$, $T = 20\,^\circ\mathrm{C}$.

It is obvious from table 8 that the proposed model is also efficient for the mono-crystalline technology since all calculated values from the dynamic algorithm have almost the same values given by the manufacturer. This error does not exceed 1%. However, the error between the manufacturing values and the calculated values from the dynamic algorithm for the amorphous panel is equal to 4% (table 9).

Table 1. Datasheet parameters of poly-crystalline, mono-crystalline and amorphous panels.

Datasheet parameter	Poly-crystalline		Mono-crystalline		Amorphous
	MSX60	KC-200GT	ISF-240	SW 280	U-EA110
I_{sc} (A)	3.8	8.21	8.46	9.71	2.5
V_{oc} (V)	21.1	32.9	37.1	39.5	71
I_{mp} (A)	3.5	7.61	7.91	9.07	2.04
V_{mp} (V)	17.1	26.3	30.3	31.2	54
K_v V/C	$-80 \cdot 10^{-3}$	$-123 \cdot 10^{-3}$	$-120 \cdot 10^{-3}$	$-118 \cdot 10^{-3}$	-0.39
K_i A/C	$3 \cdot 10^{-3}$	$3.18 \cdot 10^{-3}$	$3.5 \cdot 10^{-3}$	$3.88 \cdot 10^{-3}$	0.056
N_s	36	54	60	60	106

Table 2. MSX60 points results of dynamic algorithm data compared with results of refs. [10] and [18] and the datasheet data at STC.

Model parameter	Datasheet	Computed results by dynamic algorithm	Newton-Raphson method [10]	STC algorithm [18]
I_{ph} (A)	–	3.8	3.8084	3.8
I_{01} (A)	–	$4.6502 \cdot 10^{-10}$	$4.8723 \cdot 10^{-10}$	$4.704 \cdot 10^{-10}$
I_{02} (A)	–	$4.6502 \cdot 10^{-10}$	$6.1528 \cdot 10^{-10}$	$4.704 \cdot 10^{-10}$
R_s (Ω)	–	0.335	0.3692	0.35
R_p (Ω)	–	149.4678	169.0471	176.4
a_1	–	1	1.0003	1
a_2	–	2	1.9997	1.2
I_{sc} (A)	3.8	3.7915	3.8	3.79
V_{oc} (V)	21.1	21.0644	21.06	21.04
I_{mp} (A)	3.5	3.4824	3.493	3.49
V_{mp} (V)	17.1	17.1868	17.1	17.12
P_{mp} (W)	60	59.8520	59.76	59.76

Table 3. Kyocera KC-200GT points results of dynamic algorithm data compared with results of refs. [10] and [18] and the datasheet data at STC.

Model parameter	Datasheet	Computed results by dynamic algorithm	Newton-Raphson method [10]	STC algorithm [18]
I_{ph} (A)	–	8.21	8.2237	8.21
I_{01} (A)	–	$4.079 \cdot 10^{-10}$	$4.1437 \cdot 10^{-10}$	$4.218 \cdot 10^{-10}$
I_{02} (A)	–	$4.079 \cdot 10^{-10}$	$1.9032 \cdot 10^{-10}$	$4.218 \cdot 10^{-10}$
R_s (Ω)	–	0.312	0.3305	0.32
R_p (Ω)	–	131.689	196.5	160.5
a_1	–	1	1.0003	1
a_2	–	2	1.9997	1.2
I_{sc} (A)	8.2	8.19	8.2	8.19
V_{oc} (V)	32.9	32.8571	32.85	32.8
I_{mp} (A)	7.61	7.566	7.646	7.58
V_{mp} (V)	26.3	26.4	26.1	26.4
P_{mp} (W)	200	200.0028	199.6	200.15

Table 4. Matching points of the datasheet and two-diode model for the KYOCERA KC-200GT module at 800 W/m^2 and 20 °C.

Datasheet parameter	Datasheet measuring	Dynamic algorithm	Results of simulation of the model using R_s and R_p [10]
R_s (Ω)	–	0.4560	0.3305
R_p (Ω)	–	210.73	196.5
I_{sc} (A)	6.62	6.605	6.6
V_{oc} (V)	29.9	29.87	29.86
I_{mp} (A)	6.13	6.097	6.1
V_{mp} (V)	23.2	23.28	23.96
P_{mp} (W)	142	142.0046	146.5

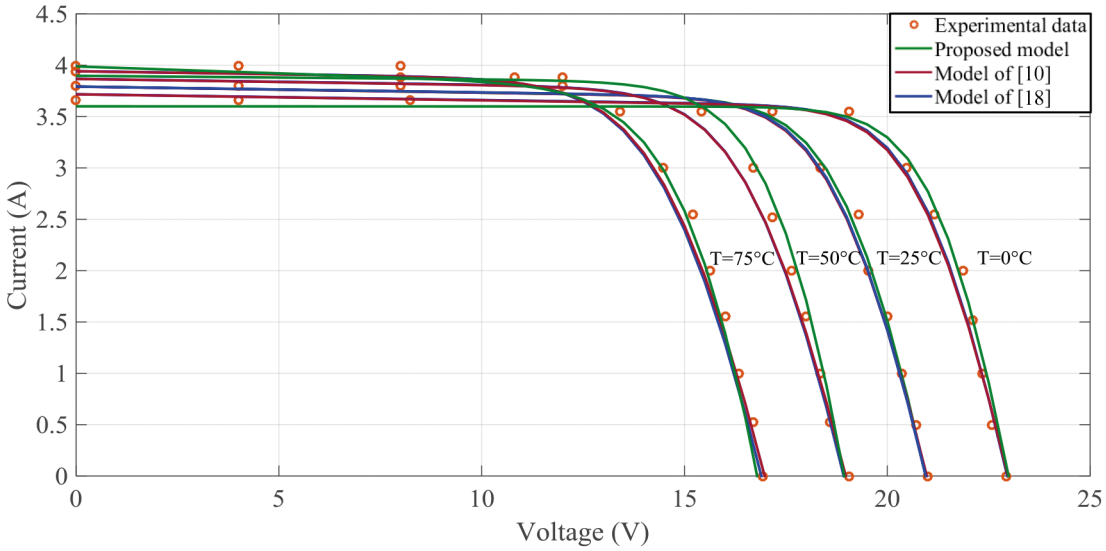

Fig. 3. *I-V* curves of MSX60 comparing between the model of refs. [10] and [18], the developed model using the dynamic algorithm and manufacturing data at various temperatures and $G = 1000$ W/m^2.

PV parameters of the datasheet are compared to those obtained with methods of ref. [10], ref. [18] and the dynamic algorithm. The series and shunt resistances of the PV panel are maintained constant in the case of the classic algorithm; thus, the error between measured and estimated PV parameters increases when climatic conditions move away from STC. Contrary to the dynamic algorithm, R_s and R_p vary *versus* both temperature and irradiance. This leads to have a PV model close to the real PV for various climatic conditions.

To evince more its efficiency and performance, the proposed five-parameter estimation method for the two-diode model is validated for the mono-crystalline SG MONO GF 170 F PV panel. Experimental data are compared to simulated ones with dynamic algorithms in fig. 6 for various climatic conditions.

In order to evaluate models performances for each climatic condition we calculate the RMSE (Root-Mean-Square Error) given by

$$\mathrm{RMSE} = \sqrt{\frac{1}{N}\sum_{i=1}^{N}(x_i - \overline{x_i})^2}, \tag{8}$$

where N is the number of obtained points, $\overline{x_i}$ is the estimated value, x_i is the observed value.

Table 10 resumes the RMSE of the dynamic algorithm for different climatic conditions. This table confirms the effectiveness of the dynamic algorithm.

It is obvious from fig. 6 and table 10 that experimental results are close to simulation results computed through the five-parameter estimation method taking into account dynamic series and shunt resistances for different climatic conditions.

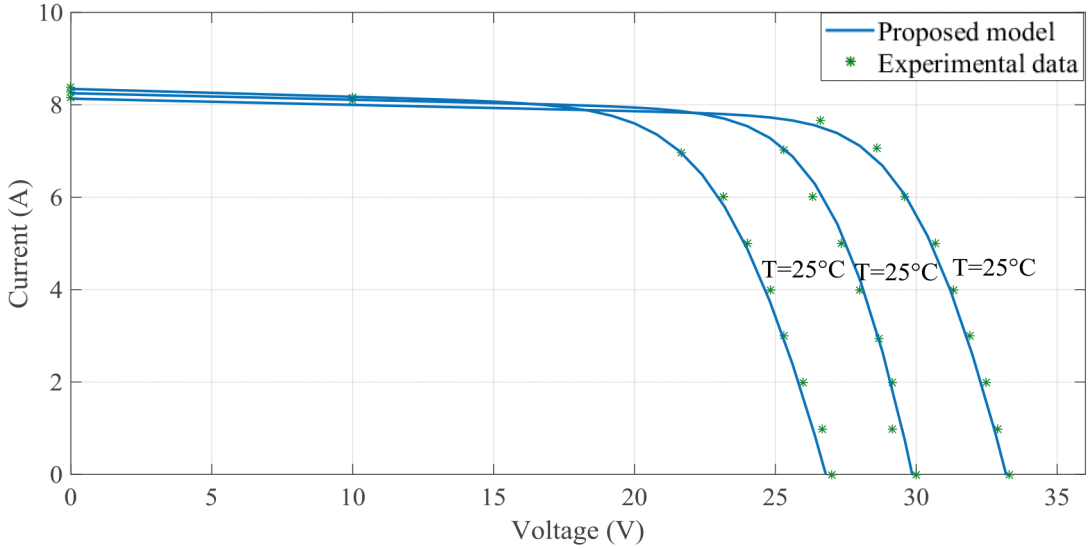

Fig. 4. I-V curves of KC-200GT at various temperatures and $G = 1000\,\mathrm{W/m^2}$.

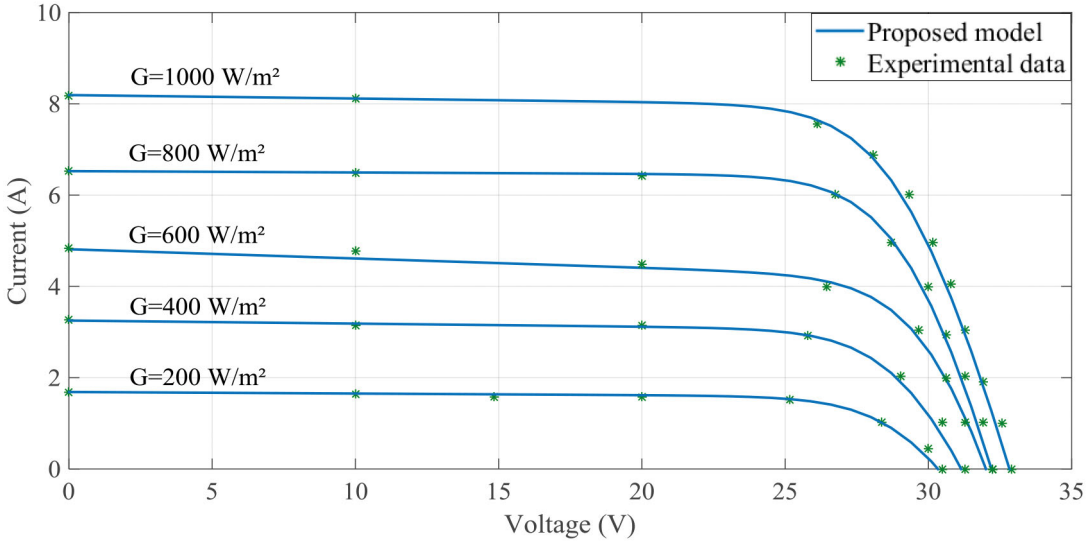

Fig. 5. I-V curves of KC-200GT at various irradiations and $T = 25\,^{\circ}\mathrm{C}$.

Table 5. Results of resistances values of KC-200GT using the dynamic algorithm for several temperatures.

$G = 1000\,\mathrm{W/m^2}$			
T (°C)	75	50	25
R_s (Ω)	0.25	0.18	0.246
R_p (Ω)	58.78	50.64	74.1

Table 6. Results of resistances values of KC-200GT using dynamic algorithm for several irradiations.

$T = 25\,^{\circ}\mathrm{C}$					
G ($\mathrm{W/m^2}$)	1000	800	600	400	200
R_s (Ω)	0.246	0.18	0.268	0.3	0.9
R_p (Ω)	74.1	102.1	49.1	121.9	226

Table 7. Computing parameters of mono-crystalline modules of the dynamic algorithm at STC.

Datasheet parameter	ISF-240	SW 280
I_{ph} (A)	8.46	9.71
I_{01} (A)	$2.95 \cdot 10^{-10}$	$7.13 \cdot 10^{-11}$
I_{02} (A)	$2.95 \cdot 10^{-10}$	$7.13 \cdot 10^{-11}$
R_s (Ω)	0.254	0.3690
R_p (Ω)	185.25	99.2735
a_1	1	1
a_2	2	2

Table 8. Computing parameters of mono-crystalline modules of the dynamic algorithm at $800\,\mathrm{W/m^2}$ and $20\,^\circ\mathrm{C}$.

Datasheet parameter	ISF-240		SW 280	
	Datasheet measuring	Dynamic algorithm	Datasheet measuring	Dynamic algorithm
R_s (Ω)	–	0.3690	–	0.395
R_p (Ω)	–	425.3552	–	196.6
I_{sc} (A)	6.81	6.8	7.85	7.83
V_{oc} (V)	33.6	33.58	36.1	36.06
I_{mp} (A)	6.37	6.35	7.33	7.27
V_{mp} (V)	26.37	26.9	28.5	28.7
P_{mp} (W)	170	170.9	209.2	209.29

Table 9. Computing parameters of the amorphous modules of the dynamic algorithm.

Datasheet parameter	U-EA110			
	STC		$G = 800\,\mathrm{W/m^2}$, $T = 20\,^\circ\mathrm{C}$	
	Datasheet measuring	Dynamic algorithm	Datasheet measuring	Dynamic algorithm
R_s (Ω)	–	1.336	–	0.01
R_p (Ω)	–	126.22	–	139.5
I_{sc} (A)	2.5	2.5	2.02	2.0199
V_{oc} (V)	71	70.3	65.5	64.677
I_{mp} (A)	2.04	2.07	1.66	1.6
V_{mp} (V)	54	55	49.2	52
P_{mp} (W)	110	114	81.8	83

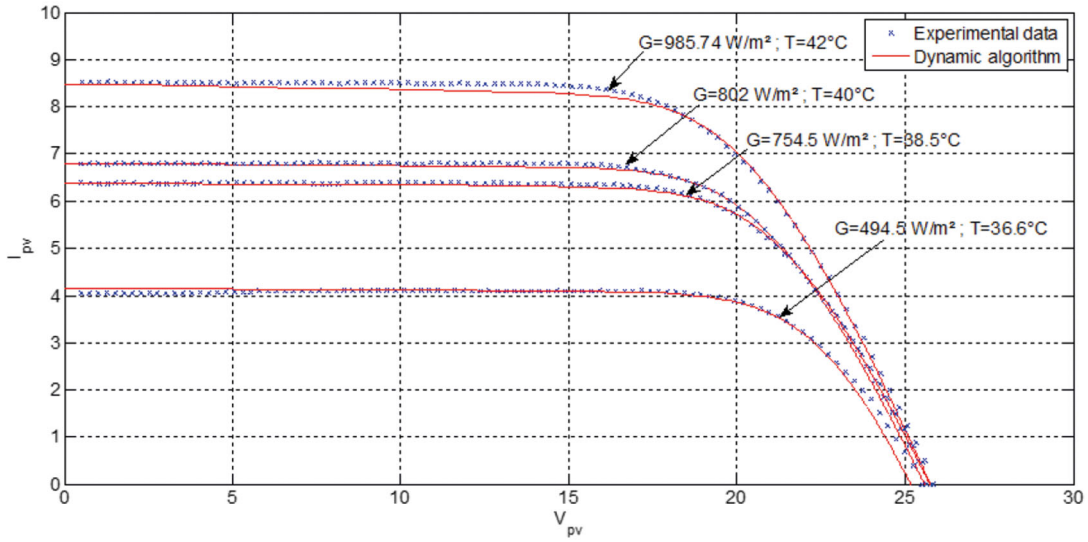

Fig. 6. *I-V* curves for various temperatures and irradiances.

Table 10. *I-V* curves error.

Climatic condition	RMSE for dynamic algorithm
$G = 754.49\,\mathrm{Wm}^{-2}$ and $T = 38.5\,^{\circ}\mathrm{C}$	0.0771
$G = 494.63\,\mathrm{Wm}^{-2}$ and $T = 36.6\,^{\circ}\mathrm{C}$	0.13629
$G = 985.75\,\mathrm{Wm}^{-2}$ and $T = 42\,^{\circ}\mathrm{C}$	0.12633
$G = 802\,\mathrm{Wm}^{-2}$ and $T = 40\,^{\circ}\mathrm{C}$	0.07465

5 Conclusion

The *I-V* characteristics of a photovoltaic PV module can be reproduced considering a two-diode model equivalent circuit made of non-linear equations. In this paper, the five unknown parameters of the considered two-diode PV model have been evaluated. Iterative algorithms are developed to estimate unknown PV parameters. The simulation results for different technologies of the PV module are summarized in tables. This table benchmarking showed that the new algorithm gives, for different manufacturing technologies of the PV cell, models curves almost overlapping with experimental ones. A particular attention has been devoted to the variation of shunt and series resistances of a PV module as they have a large impact on the efficiency of the PV module at different operating conditions. In addition the simulated *I-V* curves are compared to experimental results of a SG MONO GF 170 F proving the effectiveness and the accuracy of the dynamic algorithm when irradiance and temperature vary.

References

1. V. Khanna, B.K. Das, D. Bisht, Vandana, P.K. Singh, Renew. Energy **78**, 105 (2015).
2. V. Lo Brano, A. Orioli, G. Ciulla, A. Di Gangi, Sol. Energy Mater. Sol. Cells **94**, 1358 (2010).
3. N. Rajasekar, Neeraja Krishna Kumar, Rini Venugopalan, Sol. Energy **97**, 255 (2013).
4. T. Ikegami, T. Maezono, F. Nakanishi, Y. Yamagata, K. Ebihara, Sol. Energy Mater. Sol. Cells **67**, 389 (2001).
5. Giuseppina Ciulla, Valerio Lo Brano, Vincenzo Di Dio, Giovanni Cipriani, Renew. Sustain. Energy Rev. **32**, 684 (2014).
6. M.U. Siddiqui, M. Abido, Appl. Soft Comput. **13**, 4608 (2013).
7. Kashif Ishaque, Zainal Salam, Hamed Taheri, Simul. Modell. Pract. Theory **19**, 1613 (2011).
8. Kashif Ishaque, Zainal Salam, Hamed Taheri, Sol. Energy Mater. Sol. Cells **95**, 586 (2011).
9. Carlos R. Sánchez Reinoso, Diego H. Milone, Román H. Buitrago, Appl. Energy **103**, 278 (2013).
10. Adel A. Elbaset, Hamdi Ali, Montaser Abd-El Sattar, Sol. Energy Mater. Sol. Cells **130**, 442 (2014).
11. W. De Soto, *Improvement and validation of a model for photovoltaic array performance*, MS Thesis, Mechanical Engineering, University of Wisconsin-Madison (2004).
12. W. De Soto, S.A. Klein, W.A. Beckman, Sol. Energy **80**, 78 (2006).
13. P. Grunow *et al.*, *Weak light performance and annual yields PV modules and systems as a result of the basic parameter set of industrial solar cells*, in *19th European Photovoltaic Solar Energy Conference, 7-11 June 2004, France.*

14. D.F. Alam, D.A. Yousri, M.B. Eteiba, Energy Convers. Manag. **101**, 410 (2015).
15. C. Carrero, J. Rodrıguez, D. Ramırez, C. Platero, Renew. Energy **35**, 1103 (2010).
16. Amal Marrekchi, Souhir Sallem, Giuseppe Marco Tina, Mohamed Ben ali Kammoun, *A new five parameters estimation method for two diod model of PV module*, in *6th IREC2015 International Renewable Energy Congress* (IEEE, 2015) DOI:10.1109/IREC.2015.7110947.
17. Lotfi Khemissi, Brahim Khiari, Ridha Andoulsi, Adnane Cherif, Sol. Energy **86**, 1129 (2012).
18. K. Ishaque, Z. Salam, H. Taheri, J. Power Electron. **11**, 179 (2011).
19. Kashif Ishaque, Zainal Salam, Syafaruddin, Sol. Energy **85**, 2217 (2011).